Catalysis Today 175 (2011) 541–545

Contents lists available at ScienceDirect

Catalysis Today

journal homepage: www.elsevier.com/locate/cattod

Influence of Au particle size on Au/CeO_2 catalysts for CO oxidation

Tana, Fagen Wang, Huaju Li, Wenjie Shen*

State Key Laboratory of Catalysis, Dalian Institute of Chemical Physics, Chinese Academy of Sciences, Dalian 116023, China

ARTICLE INFO

Article history:
Available online 12 May 2011

Keywords:
Au/CeO_2
Particle size
$Au–CeO_2$ interface
CO oxidation

ABSTRACT

The Au particle size dependence of CO oxidation on Au/CeO_2 catalysts was extensively investigated. By keeping the size of CeO_2 particle to be about 12 nm, the increasing size of Au particle from 3.9 to 7.5 nm caused significant decrease in the intrinsic activity for CO oxidation. Comparative study on sodium cyanide leaching, which effectively removed the metallic gold particles but retained the cationic gold clusters in the matrix of ceria, revealed that the cationic gold species could catalyze CO oxidation only at higher temperatures, confirming the major contribution of the metallic gold particles in the Au/CeO_2 system. Therefore, it is evident that the $Au–CeO_2$ interface determined mainly by the size of Au particle plays an essential role in achieving the high reactivity.

1. Introduction

Au/CeO_2 catalysts have been widely reported to be highly active for CO oxidation [1–3], preferential oxidation of CO in rich hydrogen [4,5], and low-temperature water-gas shift (WGS) reaction [6–9]. Although it is recognized that finely dispersed gold is essentially important in achieving the high catalytic performance, the nature of the active site is still under debate, in particular regarding the cationic or metallic species. The $Au–CeO_2$ interaction, which depends strongly on the size of Au particle and the size/shape of ceria, greatly influences the catalytic performance, but several recent works have revealed that the catalytic origin of the Au/CeO_2 system is far more complex than that proposed previously [10,11].

In the case of CO oxidation, an interesting redox interplay between Au cluster and CeO_2 matrix at the interface has been recently identified, where the incorporation of cationic Au into ceria lattice leads to the formation of a $Ce_{1-x}Au_xO_{2-\delta}$ (δ takes into account the charge balance) surface phase that considerably enhanced the redox property [11]. Similarly, the high activity of Au/CeO_2 catalysts for CO oxidation has been assigned to the presence of $Au^+–OH^-$ species, the highly dispersed metallic Au species strongly interacting with defects on ceria surface [12]. Notably, Corma and co-workers [13–15] have observed a direct correlation between the concentration of Au^{3+} species and the catalytic activity in Au/CeO_2, and showed that the cationic Au species were related with the perimeter interface between the Au particle and the support and that the cationic Au species were stabilized during the course of CO oxidation. Venezia et al. [11] also proposed that the presence of small Au particles was not the main requisite for achieving high CO conversion, but the strong interaction between cationic Au and ceria might determine the particularly high activity by enhancing the ceria surface oxygen reducibility. Quite recently, however, Qian et al. [3] have concluded that the formation of Au^+ species was closely associated with and stabilized by the surface oxygen vacancy on CeO_2, but the Au^+ species alone was not active and Au nanoparticles in contact with CeO_2 were more important in catalyzing CO oxidation.

In this work, we study the effect of Au particle size in the Au/CeO_2 catalysts for CO oxidation. The size of ceria was fixed at about 12 nm while the size of Au particle was tuned by altering the temperature of calcination. It is found that the $Au–CeO_2$ interface mainly determined by the size of Au particle plays an essential role in achieving the high catalytic reactivities.

2. Experimental

2.1. Catalysts preparation

The CeO_2 support was prepared by precipitating ammonia cerium nitrate with urea in aqueous solution, as described elsewhere [16]. Briefly, 60 g of $(NH_4)_2Ce(NO_3)_6$ and 200 g of urea were dissolved into 2000 ml of water and the mixture was heated gradually to 363 K under stirring and maintained at this temperature for 27 h. After filtration and being washed with hot water, the precipitate was dried at 383 K overnight. In order to guarantee the size stability in the subsequent gold loading and reaction test, the dried solid was then calcined at 973 K for 4 h in air.

The Au/CeO_2 catalysts were prepared by a deposition–precipitation method. 13.4 g of CeO_2 powder was dispersed into 500 ml of water. The suspension was heated to

* Corresponding author. Tel.: +86 411 84379085; fax: +86 411 84694447.
E-mail address: shen98@dicp.ac.cn (W. Shen).

0920-5861/$ – see front matter © 2011 Elsevier B.V. All rights reserved.
doi:10.1016/j.cattod.2011.04.027

338 K under stirring, and 0.1 M NaOH aqueous solution was gradually added until the pH value reached 9.0. Then, 200 ml of 0.025 M $HAuCl_4{\cdot}4H_2O$ aqueous solution were added stepwise to the suspension, during which the pH value of the mixture was maintained at 9.0 by adding appropriate amounts of 0.1 M NaOH aqueous solution. The precipitate was further aged in the mother liquid for 3 h at 338 K. After filtration and being washing with hot water, the resultant solid was dried at 383 K overnight and finally calcined at 673, 773, and 873 K, yielding the Au/CeO_2-*T* materials where *T* refers to the temperature of calcination.

For comparison, the Au/CeO_2-673 and Au/CeO_2-873 samples were further treated with a 0.2 M NaCN aqueous solution for 1.5 h at room temperature in order to leach the metallic gold particles, following the procedure of Fu et al. [8]. The resulting solid was washed thoroughly with hot water, dried at 383 K and finally calcined at 573 K in air for 5 h.

2.2. Characterization

Powder X-ray diffraction (XRD) patterns of the samples were recorded on a Rigaku D/Max-RB diffractor with CuKα radiation (λ = 0.15418 nm) operated at 40 kV and 200–300 mA. The XRD patterns were recorded in both wide (20–90°) and narrow range (35–42°) with steps 5°/min and 1°/min, respectively. The average crystalline sizes were calculated by the Scherrer equation.

N_2 adsorption–desorption isotherms were recorded at 77 K using a Nova 4200e instrument (Quantachrome). Before the measurement, the sample was degassed at 573 K for 5 h. The specific surface area was calculated by a multipoint Braunauer–Emmett–Teller (BET) analysis of the N_2 adsorption isotherm.

The actual loading of gold was measured by inductively coupled plasma atomic emission spectroscopy (ICP-AES) on a Plasma-Spec-I spectrometer. 100 mg of sample were dissolved in 5 ml of aqua regia at 353 K, and the solution was diluted to 25 ml with water.

Transmission electronic microscopy (TEM) images of the samples were recorded on a FEI Tecnai G^2 F30 S-Twin microscope operated at 300 kV. The samples were ultrasonically dispersed in anhydrous ethanol, and drops of the suspension were deposited on a standard copper grid supported by thin carbon film and dried in air.

X-ray photoelectron spectroscopy (XPS) was recorded with an ESCALAB MK-II spectrometer (VG Scientific Ltd., UK) using Al Kα radiation operated with an accelerating voltage of 10 kV. The samples were pressed into a thin disc and mounted on a sample rod placed in the analysis chamber, where the spectra of C 1s, O 1s, Ce 3d and Au 4f levels were recorded. The charge effect was corrected by adjusting the binding energy of C 1s to 284.6 eV.

2.3. Catalytic evaluation

CO oxidation was conducted in a continuous-flow fixed-bed quartz tubular reactor under atmospheric pressure. 50 mg of Au/CeO_2 catalysts (40–60 mesh) were placed between two layers of quartz wool inside the reactor and pretreated with a 20%O_2/He mixture (50 ml/min) at 523 K for 1.5 h. After being cooled down to room temperature, the reaction gas (1%CO/21%O_2/He, 50 ml/min) was introduced through a mass flow controller and the temperature was programmed to rise at a rate of 10 K/min. The outlet gas was on-line analyzed by a gas chromatogram equipped with a thermal conductivity detector (TCD) and a flame ionization detector (FID).

For kinetic studies, the turnover frequency (TOF) was calculated on the basis of the number of Au atoms exposed on the surface and the conversion of CO was kept below 10% by adjusting the gas flow rate. The dispersion of gold was calculated according to the reported procedure [17]. The related parameters were taken by assuming that the Au particles had spherical or hemispherical shapes mostly exposing the {1 1 1} facet according to HRTEM observations. TOF was then calculated on the definition of the number of CO molecules converted on per Au site per second.

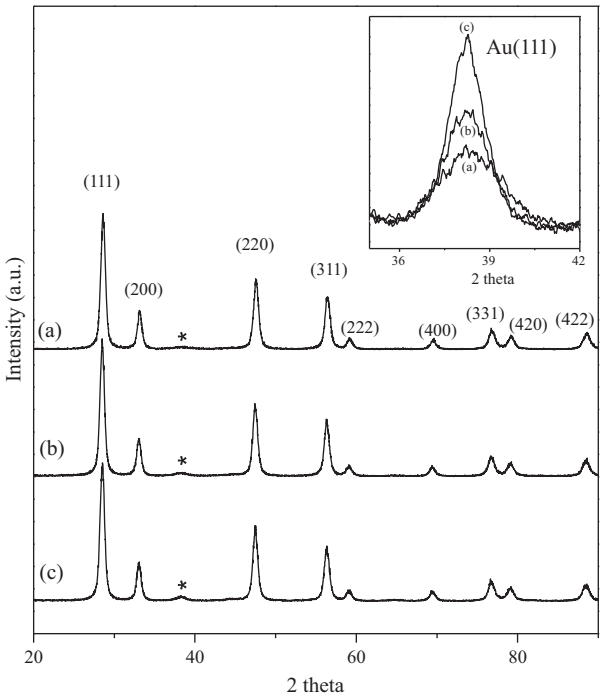

Fig. 1. XRD patterns of the Au/CeO_2-*T* catalysts: *T* = 673 K (a), 773 K (b), and 873 K (c).

3. Results and discussion

3.1. Catalyst characterization

The actual loading of Au is 3.16 wt.% determined ICP-AES analysis. The surface areas of these series of Au/CeO_2 catalysts are around 40 m^2/g. As shown in Fig. 1, the XRD patterns of the Au/CeO_2 catalysts show typical diffractions of ceria fluorite structure (JCPDS 34-0394), and the calculated grain size of ceria is about 12 nm. Weak diffractions of Au (1 1 1) are detected at $2\theta = 38.5°$. Further narrow ranged X-ray diffraction pattern indicated that the width at half-height (FWHM) of the Au (1 1 1) diffraction line alter remarkably due to the variation in Au crystalline size. The crystalline size of Au is 3.9 nm in the Au/CeO_2-673 catalyst while it increases to 6.2 and 7.4 nm in the Au/CeO_2-773 and Au/CeO_2-873 catalysts, suggesting that the size of Au grains enlarges with evaluating the temperature of calcination.

Fig. 2 shows the TEM images of the Au/CeO_2 catalysts. It is obvious that the size and the shape of the CeO_2 particles remain practically unchanged in all the samples. The CeO_2 particles are mostly in spherical shape and the size ranges from 10 to 20 nm with an average size of 12 nm, in good agreement with the XRD measurements. This can be ascribed to the previous treatment for the CeO_2 support at 973 K, which leads to a rather stable CeO_2 structure. In other words, the loading of gold and the subsequent calcination, carried out at lower temperatures, has nearly no effect on the size and shape of the CeO_2 support, making it possible to elaborate the effect of Au particle size by keeping CeO_2 particle size and shape constant. On the other hand, the size of gold particles varies largely with increasing the temperature of calcination. The mean size of Au particles is 3.9 nm in the Au/CeO_2-673 catalyst, and then increases to 5.4 nm in the Au/CeO_2-773 catalyst and finally up to 7.5 nm for

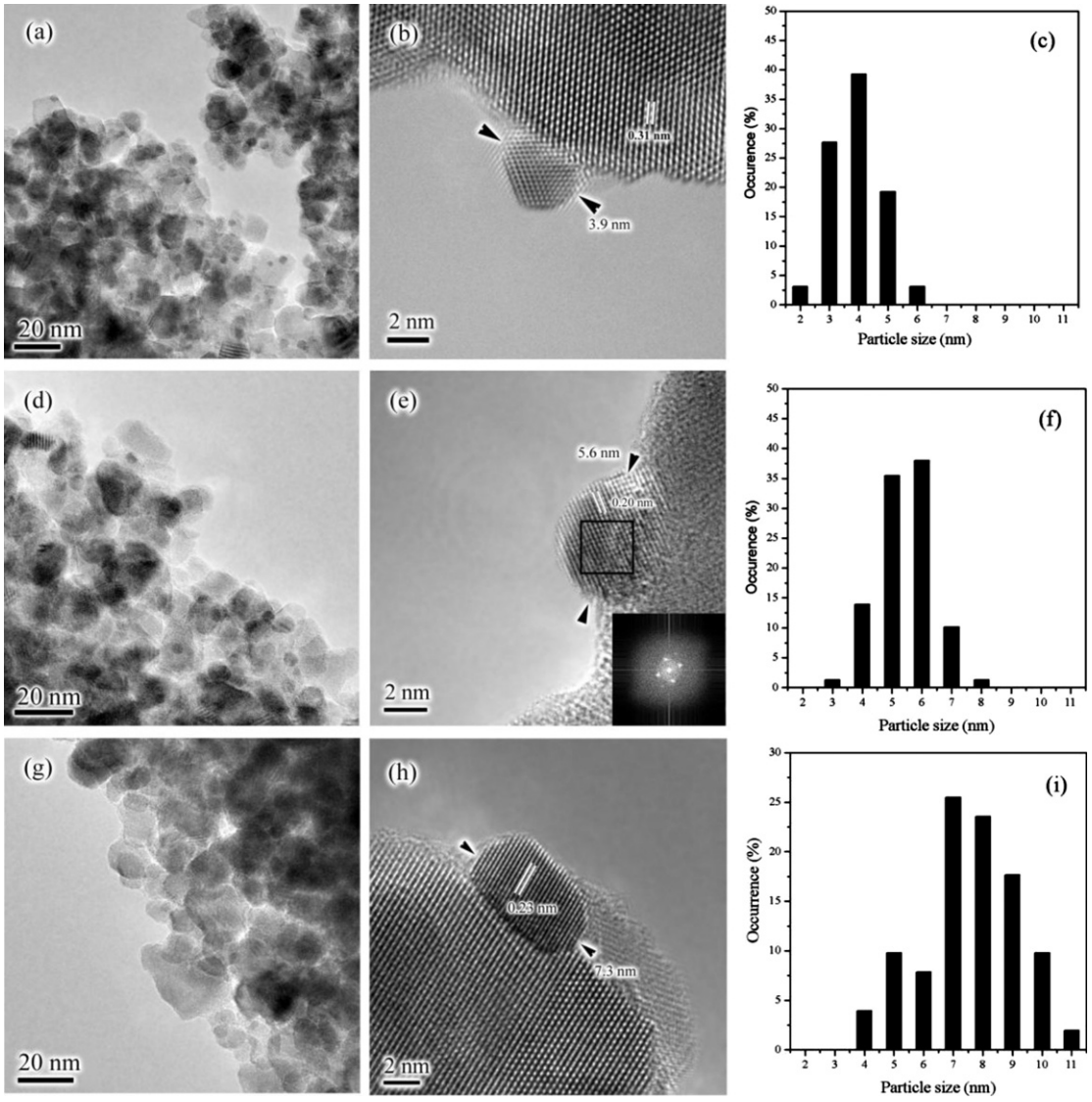

Fig. 2. TEM images and Au size distributions of the Au/CeO_2-*T* catalysts: *T* = 673 K (a–c), 773 K (d–f), and 873 K (g–i).

the Au/CeO_2-873 catalyst. Meanwhile, the size distribution of Au particles also becomes broader with increasing the temperature of calcination. The Au/CeO_2-673 catalyst shows a relatively narrow size distribution of 2–6 nm with a maximum at 4 nm, whereas the Au/CeO_2-773 catalyst has a size distribution in the range of 3–8 nm with a maximum at 5–6 nm and the Au/CeO_2-873 catalyst exhibits a wide size distribution of 4–11 nm with a maximum at 7–8 nm. The fraction of particles of 2–3 nm in diameter decreases remarkably with increasing the temperature of calcination, suggesting that small Au particles aggregate into large ones during the calcination process.

Fig. 3 shows the XPS profiles of Au 4f in the Au/CeO_2 catalysts. The binding energies of Au $4f_{7/2}$ and Au $4f_{5/2}$ are 83.6 and 87.4 eV with the spin-orbit split of 3.8 eV, characteristics of Au^0 species [18]. It is further observed that the intensity of Au 4f signal decreases with increasing calcination temperature, evidencing the enlarging of Au particles. Since the gold precursor in the precipitate is easy to decompose into Au^0 in air, calcination at above 523 K is usually sufficient enough to produce metallic gold particles [19]. For example, Au/TiO_2 samples contained only Au^0 species even at a calcination temperature as low as 473 K [20], and Au particles in Au/ZrO_2 catalysts calcined at above 523 K are solely present as metallic state [21]. Therefore, it is reasonable that the

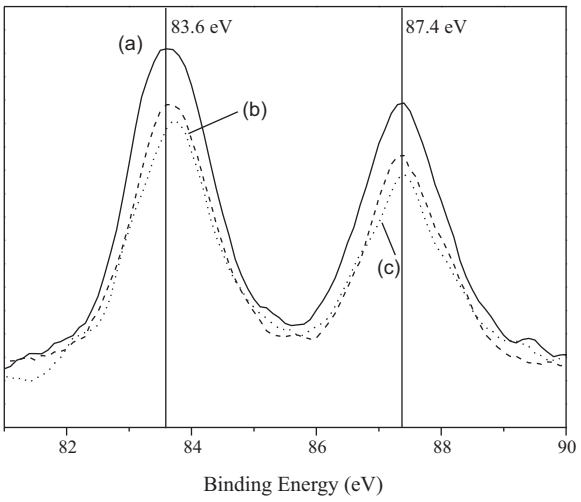

Fig. 3. XP spectra of Au 4f in the Au/CeO_2-*T* catalysts: *T* = 673 K (a), 773 K (b), and 873 K (c).

Table 1
CO oxidation results over the Au/CeO_2 catalysts.

Sample	Au/CeO_2-673	Au/CeO_2-773	Au/CeO_2-873
Au particle size (nm)	3.9	5.4	7.5
Au dispersion (%)	40	30	20
CO conv. (%)[a]	6.5	3.2	1.3
TOF ($\times 10^{-2}$ s^{-1})	6.8	4.7	2.6
Residual Au (ppm)[b]	514		1060
CO conv. (%)	2.7 (473 K), 10.1 (513 K)		1.3 (473 K), 3.7 (513 K)
TOF ($\times 10^{-2}$ s^{-1})	0.73 (437 K), 2.8 (513 K)		0.19 (473 K), 0.53 (513 K)

[a] Measured at 273 K.
[b] Measured by ICP analysis after NaCN leaching.

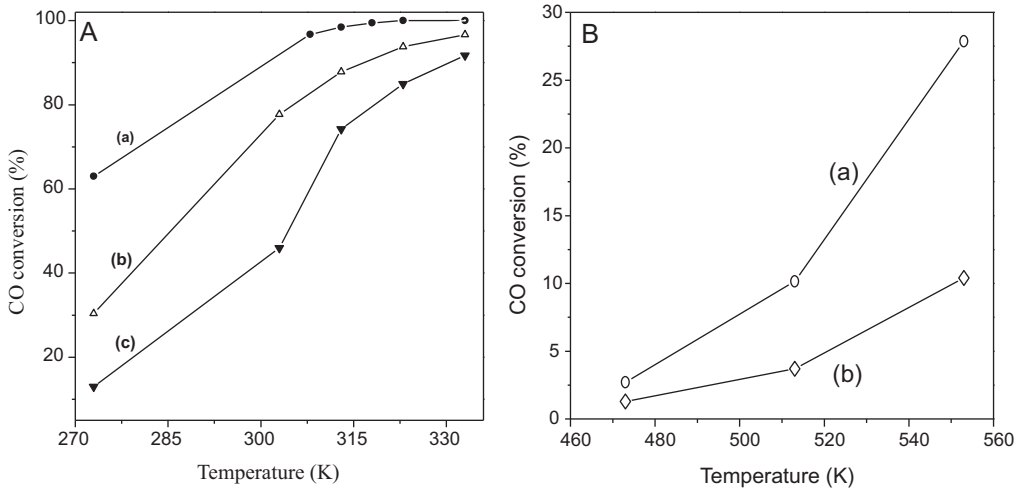

Fig. 4. CO oxidation over (A) the Au/CeO_2 catalysts with Au particle size of 3.9 nm (a), 5.4 nm (b), 7.5 nm (c) and (B) the cyanide-leached Au/CeO_2-673 (a) and Au/CeO_2-873 (b) catalysts. Reaction conditions: 50 mg catalyst sample, 1%CO/21%O_2/He, 50 ml/min.

gold particles in the Au/CeO_2 catalysts present as Au^0, almost irrespective of the particle size. Meanwhile, these are no obvious variations in the spectra of Ce 3d in the samples because of the sufficient calcination at 973 K that have readily made the surface stable.

3.2. CO oxidation

Fig. 4A shows the catalytic activities of the Au/CeO_2 catalysts for CO oxidation. Apparently, the conversion of CO strongly depends on the size of Au particle. At 273 K, the conversion of CO is readily 63% with Au particle of 3.9 nm, whereas it is only 30% and 12% for Au particles with sizes of 5.4 and 7.5 nm, respectively. The measured TOF of gold at 273 K is 6.8×10^{-2} s^{-1} at 3.9 nm and decreases to 4.7×10^{-2} s^{-1} at 5.8 nm and 2.6×10^{-2} s^{-1} at 7.5 nm, respectively, suggesting that the intrinsic activity for CO oxidation strongly relies on the size of Au particle.

This observation is in line with the general understanding that the activity of gold catalyst is very sensitive to the particle size, and the most active catalysts comprise gold primarily in a metallic state and in intimate contact with the support [22]. Small Au particles tend to contain a larger proportion of low-coordinated sites (steps, edges and corners) and/or Au clusters comprised of Au atoms bound on ceria surface [17,23], providing more active sites on the Au–CeO_2 contact boundary for an efficient adsorption of CO and a rapid surface reaction of CO with oxygen species provided by ceria. Therefore, the dramatic difference in the reaction rate of CO due to the variation in the size of gold particle suggests that the Au–CeO_2 contact boundary is the most critical factor for CO oxidation, and further evidences the size-dependent effect of Au particles where the catalytic activity is higher when the size of Au nanoparticle is smaller.

In order to identify the role of cationic Au species possibly locating in the matrix of ceria, the Au/CeO_2-673 and Au/CeO_2-873 catalysts with gold particle sizes of 3.9 and 7.5 nm, respectively, were leached with sodium cyanide. A majority of gold particles was removed and only trace of gold species retained on the surface of ceria (Table 1). Considering the initial size distribution of gold particles, the remaining gold after leaching should be very small clusters (<1 nm) probably comprised of Au atoms which are strongly associated with the surface of CeO_2. When examined for CO oxidation, however, the conversions of CO decrease significantly because of the removal of gold particles and the temperature for the occurrence of CO oxidation shifts to a much higher region, as shown in Fig. 4B. This indicates that the metallic particles contribute largely to the reaction performance. The catalyst with Au particle size of 3.9 nm still shows a higher catalytic performance after cyanide-leaching, indicating that the activity of the remaining Au clusters is closely associated with the initial Au particles probably by providing a larger Au–CeO_2 interface which should be resulted from the higher distribution for smaller Au particles. By assuming a 100% dispersion of gold in the leached samples because of the very small clusters, the TOF for the leached Au/CeO_2-673 catalyst is about 4–5 times greater than that for the leached Au/CeO_2-673 catalyst, confirming that the very small gold clusters retained in the leached samples are still closely related to the initial particle size of Au. Probably, small Au particles on the CeO_2 surface enhance the incorporation of Au ions into CeO_2 lattice, forming Au clusters that are strongly contacted with the surface cerium–oxygen bonds.

4. Conclusion

The activity of Au/CeO_2 catalysts for CO oxidation could be greatly improved by reducing the size of gold particle in the

range of 3.9–7.5 nm, which affects significantly the Au–CeO_2 contact boundary where the reaction occurs. Although the cationic gold species obtained by leaching the metallic gold particles with sodium cyanide could catalyze CO oxidation at higher temperatures, the Au–CeO_2 interface that depended strongly on the size of Au particle still contributed largely to the catalytic performance.

Acknowledgement

The financial support of this work by the National Natural Science Foundation of China (20773119, 20923001, and 21025312) is gratefully acknowledged.

References

[1] D. Widmann, R. Leppelt, R.J. Behm, J. Catal. 251 (2007) 437.
[2] V. Aguilar-Guerrero, B.C. Gates, J. Catal. 260 (2008) 351.
[3] K. Qian, S. Lv, X. Xiao, H. Sun, J. Lu, M. Luo, W. Huang, J. Mol. Catal. A 306 (2009) 40.
[4] F. Arena, P. Famulari, N. Interdonato, G. Bonura, F. Frusteri, L. Spadaro, Catal. Today 116 (2006) 384.
[5] F. Arena, P. Famulari, G. Trunfio, G. Bonura, F. Frusteri, L. Spadaro, Appl. Catal. B 66 (2006) 81.
[6] A. Karpenko, R. Leppelt, V. Plzak, R.J. Behm, J. Catal. 252 (2007) 231.
[7] Q. Fu, A. Weber, M. Flytzani-Stephanopoulos, Catal. Lett. 77 (2001) 87.
[8] Q. Fu, W. Deng, H. Saltsburg, M. Flytzani-Stephanopoulos, Appl. Catal. B 56 (2005) 57.
[9] C.H. Kim, L.T. Thompson, J. Catal. 244 (2006) 248.
[10] Z. Tang, J.K. Edwards, J.K. Bartley, S.H. Taylor, A.F. Carley, A.A. Herzing, C.J. Kiely, G.J. Hutchings, J. Catal. 249 (2007) 208.
[11] A.M. Venezia, G. Pantaleo, A. Longo, G.D. Carlo, M.P. Casaletto, F.L. Liotta, G. Deganello, J. Phys. Chem. B 109 (2005) 2821.
[12] U.R. Pillai, S. Deevi, Appl. Catal. A 299 (2006) 266.
[13] J. Guzman, S. Carrettin, A. Corma, J. Am. Chem. Soc. 127 (2005) 3286.
[14] J. Guzman, S. Carrettin, J.C. Fierro-Gonzalez, Y. Hao, B.C. Gates, A. Corma, Angew. Chem. Int. Ed. 44 (2005) 4778.
[15] P. Concepción, S. Carrettin, A. Corma, Appl. Catal. A 307 (2006) 42.
[16] W. Cai, F. Wang, E. Zhan, A.C. Van Veen, C. Mirodatos, W. Shen, J. Catal. 257 (2008) 96.
[17] S.H. Overbury, V. Schwartz, D.R. Mullins, W.F. Yan, S. Dai, J. Catal. 241 (2006) 56.
[18] E.D. Park, J.S. Lee, J. Catal. 186 (1999) 1.
[19] G.C. Bond, Gold Bull. 34 (2001) 117.
[20] R. Zanella, S. Giorgio, C.-H. Shin, C.R. Henry, C. Louis, J. Catal. 222 (2004) 357.
[21] J. Li, Tana, W. Song, E. Zhan, W. Shen, Gold Bull. 42 (2009) 48.
[22] R. Burch, Phys. Chem. Chem. Phys. 8 (2006) 5483.
[23] N. Lopez, T.V.W. Janssens, B.S. Clausen, Y. Xu, M. Mavrikakis, T. Bligaard, J.K. Nørskov, J. Catal. 223 (2004) 232.